Higher Ordered Modes in Coaxial Waveguides

The coaxial line shown below is a commonly used TEM mode waveguide, of course. This structure, however, will also support the propagation of higher-ordered TE^z + TM^z modes, which have a non-zero cutoff frequencies, in addition to the TEM mode.

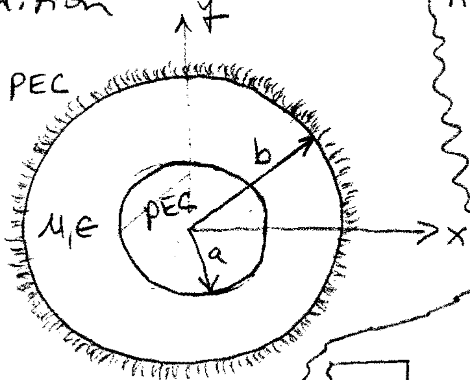

Applications of this analysis include:

1. What's the highest f for single mode operation (TEM).
2. Solving probs. including discontinuities in coaxial lines. For example:

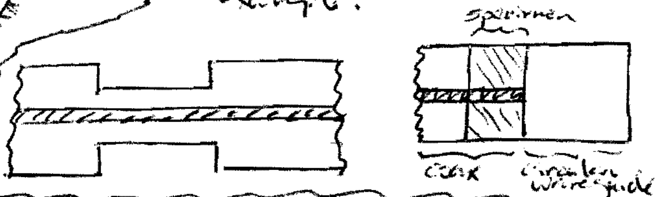

To discover these higher-ordered modes, we will solve the wave equations for E_z and H_z in the region between the conductors. This is a separable region so we expect closed form analytical solutions for the fields.

The inner conductor is concentrically located wrt the outer conductor. What if it weren't? Still separable?

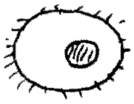

TE^z modes

We'll begin with the TE^z modes where, as we saw in the last lecture,

$$H_z = \left[A \sin(n\phi) + B\cos(n\phi)\right]\cdot\left[C J_n(\beta_c\rho) + D Y_n(\beta_c\rho)\right] e^{-j\beta_z z} \quad (1)$$

We'll only be searching for wave solutions prop. in $+z$.

Unlike as in the previous lecture, the solution domain does not include the origin where $|Y_n| \to \infty$. Consequently, we cannot discard this term as we did in a hollow circular waveguide.

The boundary conditions we need to enforce in this problem are $\hat{n}\times E = 0$ @ $\rho = a$ & b $\forall \phi$ & z. With $E_z = 0$, then E_ϕ must be determined from H_z in (1):

$$E_\phi = \frac{j\omega\mu}{\beta_c^2}\frac{\partial H_z}{\partial \rho} \underset{\substack{\uparrow \\ (1)}}{=} \frac{j\omega\mu}{\beta_c^2}\left[A\sin(n\phi) + B\cos(n\phi)\right]\cdot \frac{\beta_c}{\beta_c}\left[C\frac{\partial J_n(\beta_c\rho)}{\partial\rho} + D\frac{\partial Y_n(\beta_c\rho)}{\partial\rho}\right]e^{-j\beta_z z}$$

or

$$E_\phi = \frac{j\omega\mu}{\beta_c}\left[A\sin(n\phi) + B\cos(n\phi)\right]\cdot\left[C J_n'(\beta_c\rho) + D Y_n'(\beta_c\rho)\right]e^{-j\beta_z z} \quad (2)$$

where the prime indicates differentiation wrt the argument. Now, we'll use (2) and apply the appropriate boundary conditions:

- $\underline{E_\phi = 0 \text{ at } \rho = a}$. In order for this b.c. to be satisfied for all ϕ and z requires, from (2), that

$$C J_n'(\beta_c a) + D Y_n'(\beta_c a) = 0 \quad (3)$$

- $\underline{E_\phi = 0 \text{ at } \rho = b}$. In a similar fashion, from (2)

$$C J_n'(\beta_c b) + D Y_n'(\beta_c b) = 0 \quad (4)$$

Previously in the course when analyzing other waveguiding structures (hollow rect. waveguide and circular waveguide) we constrained β_c with an analytical equation, such as $\beta_x =$, $\beta_y =$, or $\beta_\rho =$. We can't do that here analytically.

oddly, we don't care too much about the "unknowns" C & D here. What we want to determine is β_c.

Equations (2) and (3) constitute two eqns. in two unknowns. Nontrivial solutions for C & D are possible, only when the determinant is zero. That is, in matrix form (3) & (4) are written as

$[\bar{\bar{M}}]\cdot\begin{bmatrix} C \\ D \end{bmatrix} = [\phi]$

$\begin{bmatrix} C \\ D \end{bmatrix} = [\bar{\bar{M}}]^{-1}\cdot[\phi]$

$[\bar{\bar{M}}]^{-1} = \dfrac{[\mathrm{adj}[\bar{\bar{M}}]]^{+}}{\det[\bar{\bar{M}}]}$

$$\underbrace{\begin{bmatrix} J_n'(\beta_c a) & Y_n'(\beta_c a) \\ J_n'(\beta_c b) & Y_n'(\beta_c b) \end{bmatrix}}_{[M]}\cdot\begin{bmatrix} C \\ D \end{bmatrix} = [\phi] \qquad (5)$$

If the determinant of the matrix is nonzero, then the only solution to (5) is $C=0$ & $D=0$. However, if the determinant is zero, then nontrivial solutions to (5) are possible. Hence,

$$\begin{vmatrix} J_n'(\beta_c a) & Y_n'(\beta_c a) \\ J_n'(\beta_c b) & Y_n'(\beta_c b) \end{vmatrix} = 0$$

or $$U_n \equiv \underbrace{J_n'(\beta_c a)\,Y_n'(\beta_c b) - J_n'(\beta_c b)\,Y_n'(\beta_c a) = 0}_{\text{characteristic eqn.}} \qquad (6)$$

This is an eqn. from which we can determine β_c. However, (6) is a higher-order transcendental eqn for which there are no simple analytical sol'ns.

Rather, (6) is often solved numerically. There are an infinite number of soln's to β_c in (6). These are rank ordered with the first assigned with index $m=1$, the mode with the next highest

β_c as $m=2$, and so on. For a particular, n & m we have solutions for the TE^z_{nm} mode in a coaxial waveguide.

TM^z modes

As derived in the previous lecture,

For the TM^z modes we have $H_z = 0$ and

$$E_z = \left[A \sin(n\phi) + B\cos(n\phi)\right] \cdot \left[C J_n(\beta_c \rho) + D Y_n(\beta_c \rho)\right] e^{-j\beta_z z} \quad (8)$$

For these modes, We can apply b.c.'s directly to E_z at the inner and outer conductors.

- $\underline{E_z = 0 \text{ at } \rho = a}$. To satisfy this b.c., from (8) we find

$$C J_n(\beta_c a) + D Y_n(\beta_c a) = 0 \quad (9)$$

- $\underline{E_z = 0 \text{ at } \rho = b}$. Similarly, from (8) we find

$$C J_n(\beta_c b) + D Y_n(\beta_c b) = 0 \quad (10)$$

For nontrivial solutions to (9) & (10), the determinant of these two equations must vanish:

$$J_n(\beta_c a) Y_n(\beta_c b) - J_n(\beta_c b) Y_n(\beta_c a) = 0 \quad (11)$$

This TM^z characteristic eqn. for β_c has a form similar to that for the TE^z modes in (6).

Characteristic Equations

The characteristic eqns. (6) & (11) must be solved to

Characteristic Equations

The characteristic eqns. (6) & (11) must be solved to determine the β_c for a particular mode. From (6) for TE^z modes we'll define

$$U_n(\beta_c, a, b) \equiv J_n'(\beta_c a) Y_n'(\beta_c b) - J_n'(\beta_c b) Y_n'(\beta_c a) \qquad (12)$$

and from (11) for TM^z modes we'll define

$$V_n(\beta_c, a, b) \equiv J_n(\beta_c a) Y_n(\beta_c b) - J_n(\beta_c b) Y_n(\beta_c a) \qquad (13)$$

We're interested in finding those β_c that force these equations to zero. Plots of these two fcts are shown on the next two pages for a 7-mm airline fixture where $a = \frac{1}{2}\cdot(3\,\text{mm})$ and $b = \frac{1}{2}\cdot(7\,\text{mm})$.

It appears from these plots that the mode with the lowest $\beta_c a$ (and hence the lowest cutoff frequency) is the TE_{11} mode. The first zero of U_1 has the smallest $\beta_c a$.

What we learn from these plots is that 1. there are higher ordered modes (in addition to TEM mode), 2. There are an infinite # of these modes (no surprise), and 3. We've identified the lowest, higher-ordered mode as the TE_{11}.

Ref.: • Waldron, "Theory of Guided Electromagnetic Waves," 1969.

• Cochran, "Further formulas for calculating approximate values of the zeros of ...," IEEE MTT, 1963.

6/11

U_0:

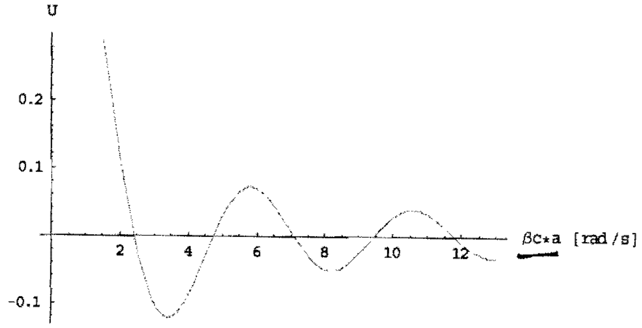

V_0:

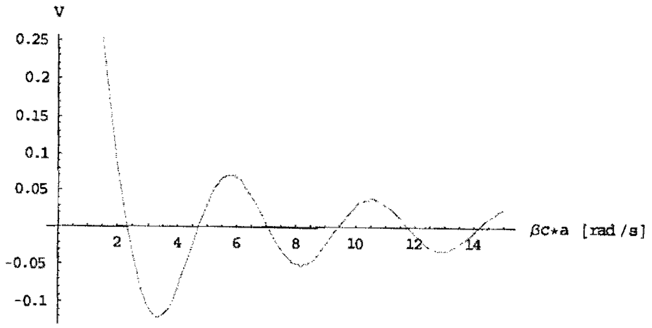

U_1:

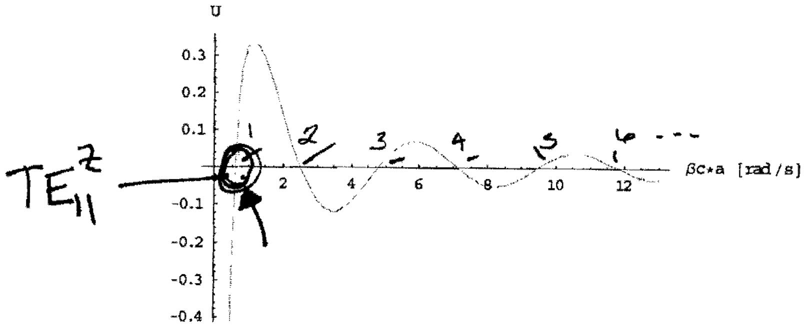

V_1:

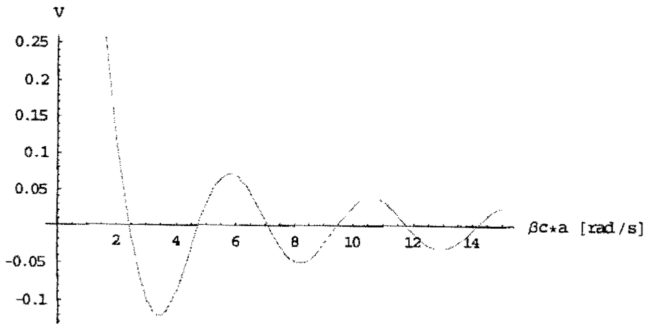

U_2:

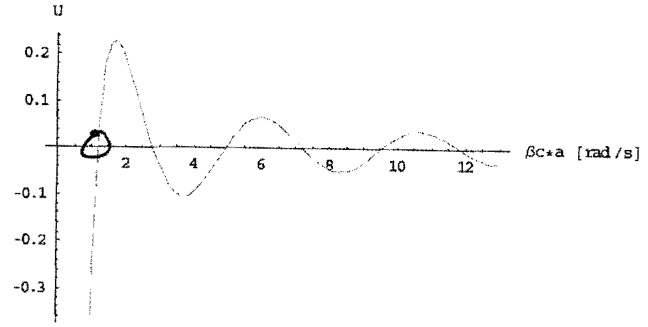
U
0.2
0.1
-0.1
-0.2
-0.3
2
4
6
8
10
12
βc*a [rad/s]

V_2:

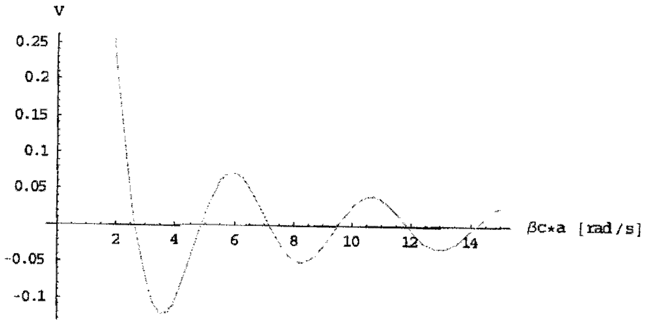
V
0.25
0.2
0.15
0.1
0.05
-0.05
-0.1
2
4
6
8
10
12
14
βc*a [rad/s]

U_3:

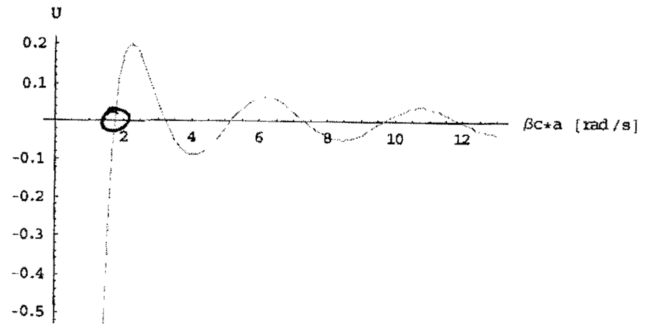
U
0.2
0.1
-0.1
-0.2
-0.3
-0.4
-0.5
2
4
6
8
10
12
βc*a [rad/s]

V_3:

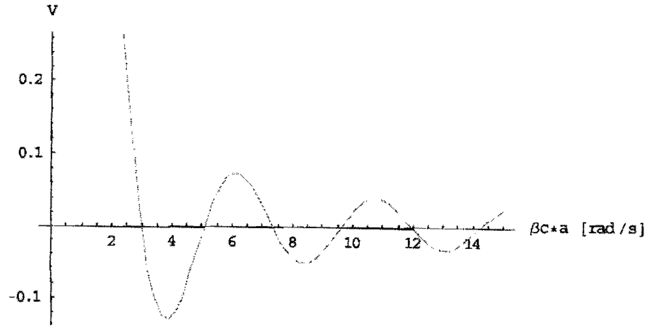
V
0.2
0.1
-0.1
2
4
6
8
10
12
14
βc*a [rad/s]

Using numerical rootfinding, the first six zeros of U_1 and V_1 are:

root #	$\beta_c a$ (from U_1 for TE^z)	$\beta_c a$ (from V_1 for TM^z)
1	0.6127	2.417
2	2.517	4.745
3	4.793	7.091
4	7.122	9.442
5	9.465	11.795
6	11.813	14.149

The mode with the lowest cutoff frequency (other than the TEM mode) we can identify from this table as the TE_{11}^z mode.

The next higher propagating mode depends on the ratio b/a, in general. For this particular example ($b = 3.5$ mm, $a = 1.5$ mm), the modes progress as: TEM, TE_{11}, TE_{21}, TE_{31}, ... The table on the following page lists the seven lowest-ordered modes in a coaxial waveguide for various ratios $\alpha \equiv b/a$

Field plot of $\bar{E}$ & $\bar{H}$ in a cross-sectional plane is shown on the following page.

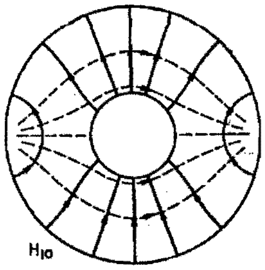

FIG. IV.8 Field patterns, in the transverse plane, of some modes of co-axial HSP waveguide. ———— E lines; --------- H lines

TABLE IV.3

CUT-OFF VALUES OF a/λ_0 FOR MODES OF CO-AXIAL HSP WAVEGUIDE

$\alpha =$ 1·0	Mode	E_{00}	H_{10}	H_{20}	H_{30}	H_{40}	H_{50}	H_{60}
	a/λ_c	0	0·159	0·318	0·478	0·637	0·796	0·955
1·2	Mode	E_{00}	H_{10}	H_{20}	H_{30}	H_{40}	H_{50}	H_{60}
	a/λ_c	0	0·174	0·348	0·522	0·695	0·869	1·042
1·5	Mode	E_{00}	H_{10}	H_{20}	H_{30}	H_{40}	H_{50}	H_{60}
	a/λ_c	0	0·192	0·384	0·575	0·764	0·951	1·136
2·0	Mode	E_{00}	H_{10}	H_{20}	H_{30}	H_{40}	E_{01}	H_{50}
	a/λ_c	0	0·216	0·427	0·630	0·824	0·994	1·009
2·5	Mode	E_{00}	H_{10}	H_{20}	H_{30}	E_{01}	H_{40}	E_{11}, H_{01}
	a/λ_c	0	0·233	0·452	0·654	0·825	0·843	0·858
3·0	Mode	E_{00}	H_{10}	H_{20}	H_{30}	E_{01}	E_{11}, H_{01}	H_{11}
	a/λ_c	0	0·245	0·466	0·663	0·739	0·781	0·839
3·5	Mode	E_{00}	H_{10}	H_{20}	H_{30}	E_{01}	E_{11}, H_{01}	H_{11}
	a/λ_c	0	0·255	0·47(5)	0·66(7)	0·688	0·73(6)	
4·0	Mode	E_{00}	H_{10}	H_{20}	E_{01}	H_{30}	E_{11}, H_{01}	H_{11}
	a/λ_c	0	0·262	0·479	0·652	0·667	0·708	0·796
4·5	Mode	E_{00}	H_{10}	H_{20}	E_{01}	H_{30}	E_{11}, H_{01}	H_{11}
	a/λ_c	0	0·26(7)	0·48(1)	0·62(7)	0·66(7)	0·68(8)	
5·0	Mode	E_{00}	H_{10}	H_{20}	E_{01}	H_{30}	E_{11}, H_{01}	H_{11}
	a/λ_c	0	0·271	0·483	0·607	0·668	0·674	0·789
5·5	Mode	E_{00}	H_{10}	H_{20}	E_{01}	E_{11}, H_{01}	H_{30}	H_{11}
	a/λ_c	0	0·27(5)	0·48(5)	0·59(2)	0·66(4)	0·67(0)	
6·0	Mode	E_{00}	H_{10}	H_{20}	E_{01}	E_{11}, H_{01}	H_{30}	H_{11}
	a/λ_c	0	0·277	0·485	0·580	0·655	0·668	0·794
6·5	Mode	E_{00}	H_{10}	H_{20}	E_{01}	E_{11}, H_{01}	H_{30}	H_{11}
	a/λ_c	0	0·27(9)	0·486	0·57(0)	0·64(9)	0·669	
7·0	Mode	E_{00}	H_{10}	H_{20}	E_{01}	E_{11}, H_{01}	H_{30}	H_{11}
	a/λ_c	0	0·282	0·486	0·560	0·644	0·670	0·80
7·5	Mode	E_{00}	H_{10}	H_{20}	E_{01}	E_{11}, H_{01}	H_{30}	H_{11}
	a/λ_c	0	0·28(4)	0·486	0·55(3)	0·64(0)	0·670	
8·0	Mode	E_{00}	H_{10}	H_{20}	E_{01}	E_{11}, H_{01}	H_{30}	H_{11}
	a/λ_c	0	0·284	0·486	0·546	0·637	0·668	0·806
∞	Mode	E_{00}	H_{10}	E_{01}	H_{20}	E_{11}, H_{01}	H_{30}	E_{21}
	a/λ	0	0·293	0·383	0·486	0·610	0·687	0·817

Note that in this table, a is the radius of the outer conductor, while

$TE_{n,m+1} = H_{n,m}$

and

$TM_{n,m} = E_{n,m}$

Reference: R. A. Waldron, *Theory of Guided Electromagnetic Waves*. New York: Van Nostrand Reinhold, 1969.

Roots to the characteristic equations (6) and (11) must be determined numerically. However, accurate approximate expressions have been presented in the literature.

In the case of the TE_{nm} modes where roots to $U_n(\chi'_{nm})=0$ are sought ($\alpha \equiv b/a$):

$$\chi'_{n,1} \approx \frac{2n}{\alpha+1}\left[1+\frac{(\alpha-1)^2}{6(\alpha+1)^2}\right] \qquad (14)$$

$$\chi'_{n,m} \approx \left[\frac{(m-1)^2\pi^2}{(\alpha-1)^2}+\frac{4n^2+3}{(\alpha+1)^2}\right]^{1/2} \qquad m=2,3,4,\cdots \qquad (15)$$

while for the TM_{nm} modes where roots to $V_n(\chi_{nm})=0$ are sought:

$$\chi_{n,m} \approx \left[\frac{m^2\pi^2}{(\alpha-1)^2}+\frac{4n^2-1}{(\alpha+1)^2}\right]^{1/2} \qquad m=1,2,3,\cdots \qquad (16)$$

For $n=1$, the following values from (14)–(16) can be compared to those on p. 8, where $\alpha = \frac{b}{a} = 2.333$:

root # = m	$\chi'_{1,m}$		$\chi_{1,m}$	
1	0.616	(14)	2.413	
2	2.486		4.741	
3	4.779		7.088	(16)
4	7.113	(15)	9.439	
5	9.458		11.792	
6	11.808		14.147	

These approximate values are very close to those

These approximate values are very close to those obtained using numerical root finding.

One important fact we can determine from the approximate expression (14) is the upper frequency for single mode (TEM) operation. From (14) for the TE_{11} mode ($n=1$):

$$\chi'_{1,1} = \beta_{c1,1} a \approx \frac{2}{\alpha+1}\left[1 + \frac{(\alpha-1)^2}{6(\alpha+1)^2}\right] \qquad (17)$$

Recall that $$\beta_c^2 + \beta_z^2 = \beta^2 = \omega^2 \mu\epsilon \qquad (18)$$

At the cutoff frequency of a particular mode, $\beta_{zmn} = 0$. Using this in (18) and substituting (17)

$$f_{c1,1} = \frac{\beta_{c1,1}}{2\pi\sqrt{\mu\epsilon}} \approx \frac{1}{\pi a(\alpha+1)\sqrt{\mu\epsilon}}\left[1 + \frac{(\alpha-1)^2}{6(\alpha+1)^2}\right] \qquad (19)$$

This expression is often further approximated by keeping only the first term:

$$f_{c1,1} \approx \left[\pi\sqrt{\mu\epsilon}\,(a+b)\right]^{-1} \qquad (20)$$

In the case of the 7-mm airline example ($a = 1.5$mm, $b = 3.5$mm)

$$f_{c1,1} \approx 19.09 \text{ GHz}$$

Leaving a 5% "buffer" gives an upper freq $\approx$ 18.13 GHz.

CONCLUSION

Unlike hybrid modes, the pure TM and TE modes have a minimum value of d/λ_0 for which they are bound to the rod. For values of d/λ_0 smaller than this, the modes are neither bound to the rod nor will propagate independently of it, hence are effectively cut off. This shows on the graphs as a nonzero slope for the curves at $\lambda/\lambda_0=1$, the respective values of d/λ_0 being given by (6) for the TM modes and by

$$[d/\lambda_0]_{\substack{\text{Dominant Mode}\\ \text{C.O.}}} = 2.405[1/\pi][K_T - 1]^{-1/2} \quad (7)$$

for the TE modes.

The asymptotic value of λ/λ_0 for large d/λ_0 is given by (5) for both TM and TE modes and is the value of λ/λ_0 that the modes would have in a dielectric medium of infinite extent.

It can be seen that any value of λ/λ_0 between 1 and $[K_T]^{-1/2}$ may be selected by proper choice of d/λ_0; however, as d/λ_0 becomes smaller, more of the energy of the wave is propagated outside the rod. In general, an increase in dielectric constant has the opposite effect of binding the wave more tightly to the rod. Since the microwave index of refraction may be varied from 1 to $[K_T]^{1/2}$, which is generally higher for a given dielectric than the respective optical index of refraction, one can almost always effect a match of velocities in an optical-microwave type experiment.

ACKNOWLEDGMENT

The authors are indebted to G. S. Heller and R. H. Kingston for many valuable discussions.

Correspondence

Further Formulas for Calculating Approximate Values of the Zeros of Certain Combinations of Bessel Functions*

INTRODUCTION

In a recent letter Gunston[1] has presented a wonderfully simple approximate formula for the smallest z zero of the Bessel function equation

$$J_p(z)N_p(kz) - J_p(kz)N_p(z) = 0 \quad (1)$$

where J_p and N_p are, respectively, the Bessel functions of the first and second kinds of real-order p. This communication is intended to draw attention to the existence of similar approximate formulas for both the larger z zeros of (1) and the roots of the equally-important companion equation

$$J_p'(z)N_p'(kz) - J_p'(kz)N_p'(z) = 0 \quad (2)$$

where $'$ indicates differentiation.

BACKGROUND

In the usual physical cases of interest the parameter p is an arbitrary real number while k is generally positive. It is known that under these conditions the zeros of (1) as a function of z are all real, simple (see Gray and Mathews[2]) and infinite in number, and these results can be extended to the z zeros of (2) (see Cochran[3]). Furthermore, since both (1) and (2) are unaffected by replacing either z by $-z$ or p by $-p$, attention need only be addressed to the case of positive values.

As pointed out by Kline[4] and Waldron[5] the solutions of equations (1) and (2) approach those of the equations $J_p(kz)=0$ and $J_p'(kz)=0$, respectively, with increasing k or p. The latter author even indicates the regions among his tabulated values in which this approximation may be reasonably made. Moreover, the familiar asymptotic expressions of McMahon[6] suffice for the calculation of the roots of both (1) and (2) whenever the quantity $\beta = S\pi/(k-1)$ is appreciable, where S is the number of the root when arranged in order of magnitude. As cogently discussed by Waldron,[5] it is convenient to index the roots of the primed equation (2) beginning with $S=0$ rather than with $S=1$ as one does for the solutions of (1). This not only obviates the difficulty wherein, under the usual numbering scheme, the McMahon expression with $\beta = S\pi/(k-1)$ gives the asymptotic expansion for the $(S+1)$st root of (2), but it also serves to set apart the fundamentally different group of roots corresponding to $S=0$. When $p=0$ these special zeros of (2) do not occur; on the other hand, for $p>0$ a representation in terms of powers of $(k-1)/\sqrt{4k}$ has been derived for them by Buchholz.[7]

FORMULAS

Let z and z' denote roots of the unprimed equation (1) and of the primed equation (2), respectively, and let δ be a positive constant. If $\delta \equiv (k-1)z$ or $\delta \equiv (k-1)z'$, the author has recently developed asymptotic expressions for the Sth zeros of (1) and (2) in the following form:

$$\left\{ \begin{matrix} z_{p,S} \\ z'_{p,S} \end{matrix} \right\} = \frac{p\delta}{\sqrt{\delta^2 - (S\pi)^2}} - \frac{\delta}{2} + \frac{1}{p} \left\{ \begin{matrix} a(\delta, S) \\ b(\delta, S) \end{matrix} \right\} + 0(p^{-2}). \quad (3)$$

The functions $a(\delta, S)$ and $b(\delta, S)$, whose precise nature need not concern us here, are independent of p. Solving for $z_{p,S}$ or $z'_{p,S}$ using the first two terms of the expansion yields

$$\left\{ \begin{matrix} z_{p,S} \\ z'_{p,S} \end{matrix} \right\} \approx \sqrt{\frac{(S\pi)^2}{(k-1)^2} + \frac{4p^2}{(k+1)^2}} \quad (4)$$

and

$$z'_{p,0} \approx 2p/(k+1).$$

* Received June 27, 1963.

[1] M. A. R. Gunston, "A simple formula for calculating approximate values of the first zeros of a Combination Bessel function equation," IEEE TRANS. ON MICROWAVE THEORY AND TECHNIQUES (*Correspondence*), vol. MTT-11, pp. 93–94; January, 1963.

[2] Gray and Mathews, "Bessel Functions," MacMillan and Co., London, p. 82; 1922.

[3] J. A. Cochran, "Remarks on the zeros of $J_p(z)Y_p(kz) - Y_p(z)J_p(kz)$ and $J_p'(z)Y_p'(kz) - Y_p'(z)J_p'(kz)$," (to be published).

[4] M. Kline, "Some Bessel equations and their application to guide and cavity theory," *J. Math. Phys.*, vol. 27, pp. 27–48; April, 1948.

[5] R. A. Waldron, "Theory of the helical waveguide of rectangular cross-section," *J. Brit. IRE*, vol. 17, pp. 577–592, October, 1957.

[6] J. McMahon, "On the roots of the Bessel and certain related functions," *Ann. Math.*, vol. 9, pp. 23–30; October; 1894.

[7] H. Buchholz, "Reihenentwicklungen für eine Determinante mit Zylinderfunktionen," *Z. Angew. Math. Mech.*, vol. 29, pp. 356–367; November, 1949.

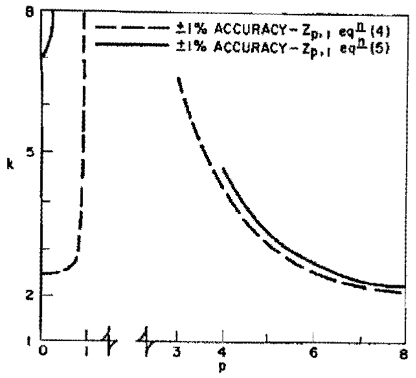

Fig. 1—Accuracy graph of the approximate formulas for $z_{p,s}$ with $s=1$.

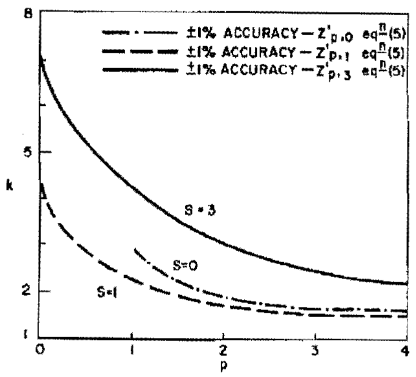

Fig. 2—Accuracy graph of the approximate formula for $z_{p,s}'$ with $s=0$, 1, and 3.

Setting $S=1$ in (4) gives Gunston's result.

It is known, though, that for given p, the roots of (1) and (2) do not coincide so it would be helpful if our simple formulas exhibited this difference. Using the full right-hand side of (3) above does yield dissimilar, but rather complex, results. By retaining only the most essential terms, however, these expressions can be approximately reduced to

$$z_{p,S} \approx \sqrt{\frac{(S\pi)^2}{(k-1)^2} + \frac{4p^2-1}{(k+1)^2}}$$

$$z'_{p,S} \approx \sqrt{\frac{(S\pi)^2}{(k-1)^2} + \frac{4p^2+3}{(k+1)^2}}$$

$$(S = 1, 2, 3, \cdots)$$

$$z'_{p,0} \approx \frac{2p}{(k+1)}\left[\frac{1+(k-1)^2}{6(k+1)^2}\right]. \quad (5)$$

For large S or small $(k-1)$ these formulas give rise to the leading terms in the asymptotic expansions of McMahon and Buchholz, and consequently the expressions of (5) become increasingly more accurate in these regions.

Following Gunston, accuracy graphs may be roughly constructed for the above simple approximate formulas. For values of (k, p) lying below the curves of Fig. 1 the formulas of (4) and (5) for $z_{p,1}$ are within ± 1 per cent of the exact value. Fig. 2 shows similar curves for $z'_{p,0}$, $z'_{p,1}$, and $z'_{p,3}$ from (5).

It is unfortunate that known existing data (see Waldron[8] and Fletcher, *et al.*[9]) does not permit us to readily compare *carefully* the approximate with the exact roots for a wider range of values of (k, p). In particular, the precise general accuracy of the expressions for $z_{p,S}$ of either (4) or (5) is somewhat uncertain for moderate p and k, say $1<p<3$ and $k>3$, and the situation is therefore not quite as depicted in Fig. 1 of Gunston.[1,9] Nevertheless, it is hoped that the two figures presented here do serve to illustrate the general regions of applicability of the formulas of (4) and (5) as either reasonable approximate values of the roots in question, or as initial approximations in computational schemes for the zeros of these important combinations of Bessel functions.

J. A. Cochran
Bell Telephone Labs., Inc.
Whippany, N. J.

[8] A. Fletcher, *et al.*, "An Index of Mathematical Tables," Addison-Wesley, Reading, Mass., 2nd ed., vol. 1, pp. 413, 414, 416; 1962.
[9] For instance, the inaccuracy of Gunston's formula for $p=5/2$, $k=3$, 4, or 5 is of the order of 2 or 3 per cent rather than less than 1.5 per cent as his figure indicates.

Transmission Line Measurement of Narrow Linewidth Ferromagnetic Samples*

Measurement of ferromagnetic resonance linewidths over a range of microwave frequencies is facilitated by the use of a nonresonant waveguide system. The loading effect encountered in such a transmission line system, however, becomes significant when the linewidth is less than a few tens of oersteds. The effect of transmission line loading was avoided by the use of an automatic compensation network.

An idealized model of the experimental system is illustrated in Fig. 1. Scattering-matrix theory is applied to the junction that is inside the balloon-like simply connected region. The test sample is placed topologically outside the junction by means of a connecting tube. If the radius of the connecting tube is small enough, the tube itself will not be significant and we have a three-port function which fits the usual simplifying assumptions of scattering matrix theory. Ports Nos. 1 and 2 are terminals of waveguide in which only the dominant mode is propagating. Port No. 3 is the surface which

* Received July 1, 1963.

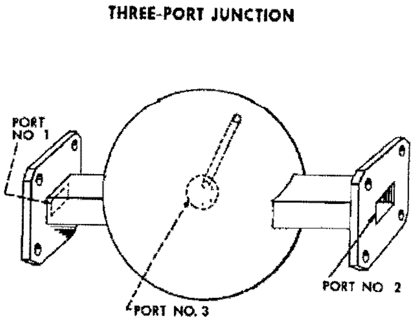

Fig. 1—Schematic view of the test section.

surrounds the test sample. The treatment of this problem is simplified by including only one mode of propagation at port No. 3. This propagating mode is closely related to the radiation field associated with the resonant mode of the sample.

It is necessary to consider the properties of the test section in terms of the signals observable at ports Nos. 1 and 2 alone. The only dissipative element in this system is the load at port No. 3. The reflection coefficient of the load at port No. 3 is written in impedance form for convenience, $(1-z)/(1+z)$. If first order perturbation theory can be used to describe a magnetic sample in the waveguide the impedance is proportional to the susceptibility.

In order to describe this three-port junction in matrix formalism, it is sufficient to identify the ports with elements of a column matrix, the amplitude and phase at each port being represented by a corresponding element. The scattered waves, also described by a column matrix, are related to the incident waves by a square matrix. Terminating the third port of the network by a reflective load reduces the order of system. The resultant two-port junction is described by a 2×2 matrix T, given in (1), which is not, in general, a unitary matrix.

$$T = \begin{bmatrix} \dfrac{(s_{11}-s_{22}^*)+(s_{11}+s_{22}^*)z}{(1-s_{33})+(1+s_{33})z} & \dfrac{(s_{12}+s_{21}^*)+(s_{12}-s_{21}^*)z}{(1-s_{33})+(1+s_{33})z} \\ \dfrac{(s_{21}+s_{12}^*)+(s_{21}-s_{12}^*)z}{(1-s_{33})+(1+s_{33})z} & \dfrac{(s_{22}-s_{11}^*)+(s_{22}+s_{11}^*)z}{(1-s_{33})+(1+s_{33})z} \end{bmatrix}. \quad (1)$$

The impedance at the third port appears in the reduced matrix T in the numerator of each term and in the common denominator of the entire matrix. A resonant condition is described by this matrix if the denominator vanishes. This, however, represents decoupling of the third port from all other ports and is of no interest in this study. The complex conjugate form arises because S is a unitary matrix; the form written here is for $+1$ value of the determinant of S.

It is useful to note at this point that: 1) Since signal is applied at one port only, the transmitted and reflected signals are the most easily observed quantities. 2) Since the sample has a narrow linewidth, the condition $z=0$ can be used for a convenient reference, the measurement being made far from resonance.

Error? Should read:

$$z'_{p,0} \approx \frac{2p}{k+1}\left[1+\frac{(k-1)^2}{6(k+1)^2}\right]$$